communications materials

Article

https://doi.org/10.1038/s43246-024-00712-z

Gelatin-based spray for forest fire prevention and fertilization

Check for updates

Yuanfang Ai[1], Na Zheng[2], Wenbo Liu[3], Ping Yang[4], Xi Wu[1], Yichen Tian[1], Chuyi Wang[1], Heyang Liu[3] ✉, Chongping Huang[4], Zhongli Liang[5], Feng Zhu[5], Longcheng Tang[6], Nanbiao Ye[7], Jianjun Li[7] & Kun Cao[1,2] ✉

Frequent forest fires, driven by hotter and drier climates, threaten biodiversity and human health, causing significant economic losses, air pollution, soil erosion, and degeneration. Current active and passive fire protection methods often suffer from environmental pollution, poor flexibility, and limited availability in remote areas. However, fast-acting surface flame retardants for passive forest fire protection, particularly for foliage, are rare. Herein, we report an easily obtainable gelatin-based fire spray, which resulted in 1.8 and 16.3-fold extension in ignition time, 34% and 39% reductions in total heat release, 78% and 92% reductions in fire growth index for dead and fresh leaves, respectively. After the fire warning is suppressed, for instance by rain, the sprayed substances can decompose and provide nitrogen and phosphorus as leaf and soil fertilizers without affecting soil microbial function, which increase plant net photosynthesis by 84% and effective nitrogen and phosphorus by 664% and 140%, respectively. Our green flame retardant and fertilizer material allows for simultaneous tree fire protection and growth.

In recent years, forest fires have caused major environmental issues and jeopardized human beings and wildlife, as they quickly became uncontrollable and difficult to address[1–7]. According to the Global Wildfire Information System (GWIS), global forest fires in 2023 destroyed nearly 400 million hectares of land and caused more than 250 deaths. In China alone, 328 forest fires occurred, victimizing about 0.4 million hectares of forest[8]. There are various strategies for vegetation fire prevention, such as the establishment of protective forests, the development of fire monitoring systems[9], the research of fire extinguishing agents and equipment[10], and education and regulation[11]. Besides, isolation belts can block fires but require large areas of land, time for maintenance, and lack flexibility, making them challenging to implement in remote areas. The most direct way is the application of extinguishing agents. Typically, they are aqueous solutions containing flame-retardant additives or powdered chemicals. This brings with it other problems, in particular, the environmental impact of chemical additives[12,13]. Therefore, it is essential to find a measure that is highly fire-efficient and environmentally friendly.

Surface flame-retardant modification is a simple and convenient way to improve the fire-retardant properties of a material without altering its internal composition[14–17]. However, few works have focused on opaque flame-retardant coatings for wood[18] and dead grass[19] to extend ignition time and improve flame retardancy. Can we put "The Emperor's New Clothes" as an invisible "fire suit" on the forest? This "fire suit" must possess three key features: (1) being nontoxic and pollution-free, (2) harmless to the growth of trees and the environment, and (3) effective fire prevention. These requirements restrict the choice of ingredients to natural or nontoxic materials suitable for large-scale application. We selected water-soluble gelatin, urea, and phytate (PAPEG), which had nitrogen- and phosphorus-based flame-retardant effects[20,21]. The mass ratio of the blends of gelatin, PAPEG, and urea was 1:0.5–1:0.5–1 to obtain the gelatin-based precursor. The performances of the sprays with different ratios were examined (Supplementary Fig. 1). And the optimal formulation, with exceptional transparency and flame retardancy, was found to be a 1:0.5:0.5 ratio of gelatin, PAPEG, and urea.

Results and discussion

Preparation and application

The design of the bio-based flame-retardant spray (FRS) was both simple and clever. Gelatin was employed as the backbone of the film and formed a

[1]Institute of Polymerization and Polymer Engineering, Zhejiang University, Hangzhou, China. [2]State Key Laboratory of Chemical Engineering, College of Chemical and Biological Engineering, Zhejiang University, Hangzhou, China. [3]School of Environmental and Natural Resources, Zhejiang University of Science and Technology, Hangzhou, Zhejiang, China. [4]Agricultural Experiment Station, Zhejiang University, Hangzhou, China. [5]Hangzhou JLS Flame Retardants Chemical Co. LTD., Hangzhou, China. [6]Key Laboratory of Organosilicon Chemistry and Material Technology of Ministry of Education, Hangzhou Normal University, Hangzhou, China. [7]State Key Laboratory of High-quality Utilization of Polymer Material Resources, Kingfa Sci&Tech Co. LTD., Guangzhou, China. ✉e-mail: heyang.liu@zust.edu.cn; kcao@che.zju.edu.cn

cross-linked network with PAPEG and urea through multiple noncovalent interactions (Fig. 1a). PAPEG was synthesized via esterification of phytic acid (PA) and polyethylene glycol 200 (PEG200), confirmed by FTIR (Supplementary Fig. 2a) and ^{31}P NMR spectra (Fig. 1a), demonstrating decreased acidity[22]. Then PAPEG and urea were homogeneously mixed with gelatin solution at room temperature. After spraying and drying, the flame-retardant coating was obtained. The phosphorus signal clearly shifted after blending with gelatin and urea, illustrating that intermolecular interactions occurred during the mixing process. It is probably because nucleophilic P=O was able to form hydrogen bonds with -NH_2/-NH-/-OH, in addition to a very small amount of unreacted P-OH, which is susceptible to ionic forces with a primary amine, as evidenced by the results of XPS (Supplementary Fig. 2a, c)[23,24]. As shown in Fig. 1a, this is evidenced by the redshift of the in-plane bending vibrational of -NH_2 in urea and the blueshift of P=O[25]. Hydrogen bonds and electrostatic interactions were formed among gelatin, PAPEG, and urea. Thereby, they were dispersed evenly in the phase diagram of atomic force microscopy (AFM), and a coated surface with very low roughness was also observed, as shown in Fig. 1c.

Before the application of FRS to trees, its safety for nontarget organisms was demonstrated by the CCK-8 cell viability assay of L929 cells. L929 cells were incubated for 48 h in a culture medium at different concentrations of FRS, and their survival rate was almost 100% in Fig. 2b, which means that the gelatin-PAPEG-urea is not toxic to mammalian cells and can be used safely. Subsequently, we sprayed the FRS onto the leaves, and the underground texture through the glossy coating (thickness of ~700 nm) was clearly observed in digital photos of samples (Fig. 1d). This was attributed to a light transmission of up to 89.1% and a haze of only 2.8% as observed in Fig. 1e. SEM images revealed that after the plants were sprayed with the gelatin-based flame retardant, a smooth and uniform film covered the leaves (Fig. 1f). In comparison, the dead leaves with more N, O, and P attached to the leaves in the EDS mapping, had smoother surface than fresh ones (Supplementary Fig. 2b). Compared to fresh leaves, fallen leaves were dehydrated and more likely to absorb FRS, as investigated by the lower contact angle (CA) of FRS on MC surface by comparison with that of OFO (Fig. 1g). Due to the intermolecular interaction between FRS and H_2O, the surface tension of FRS solution reduced by 12.2 mN m^{-1}, as well as the CA on the OFO surface. Consequently, FRS was prone to spread out over the leaf (Supplementary Fig. 2d). For a more pronounced effect, we dropped FRS on a superhydrophobic surface (lotus leaf). The water droplets contracted more easily and bounced from 31 ms to 40 ms, while the FRS droplets contracted more slowly at 31 ms and were not enriched (Fig. 1h). This behavior minimized dripping and splashing during spraying, thereby improving the utilization efficiency of FRS.

Fire protection properties

To examine the fire protection properties, we built a custom-made combustion device to observe the burning and monitor the temperature with a digital camera (Supplementary Fig. 3a). Because of the small and dry leaves and the richness of the resin, untreated LN ignited within 2 s (Fig. 2a and Supplementary Movie 1). The fire spread rapidly, generating substantial amounts of smoke and reaching temperatures above 800 °C, with minimal char remaining (Supplementary Fig. 3b). LN2.5 also burned, but it was combusted more slowly with a smaller area than did leaves without FRS (Supplementary Fig. 3c). LN5.0 burned for only 13 s after removing the flame, and temperature was below 300 °C during combustion and dropped rapidly to less than 100 °C after 35 s. Similarly, MC5.0 could self-extinguish within 20 s after being exposed to flame for 5 s, and the temperature downed to 150 °C at 35 s (Fig. 2b and Supplementary Movie 2). Fresh leaves containing a large amount of water should be difficult to ignite. We exposed the leaves to butane flame (~1100 °C) for 30 s twice. In both the OFT and OFO, the presence of FRS dramatically shortened the self-extinguishing time of the leaves and slowed the spread of fire, leading to less heat release and lower temperatures (Fig. 2c, d, Supplementary Fig. 3d, and Supplementary Movies 3–4).

In the cone calorimeter test (CCT) (Fig. 2e and Supplementary Table 1), the introduction of FRS delayed the time to ignition (TTI) for fallen leaves, especially 90 s longer for MC5.0 than for MC0. Similarly, the peak heat release rate (PHRR) was slower, indicating that FRS made the leaves more resistant to ignition and combustion. This is consistent with the earlier combustion results. Compared with those of leaves treated with water, the PHRR of LN5.0 and MC5.0 significantly decreased by 40% and 66%, respectively. This resulted in an ultralow fire performance index (FPI, TTI/

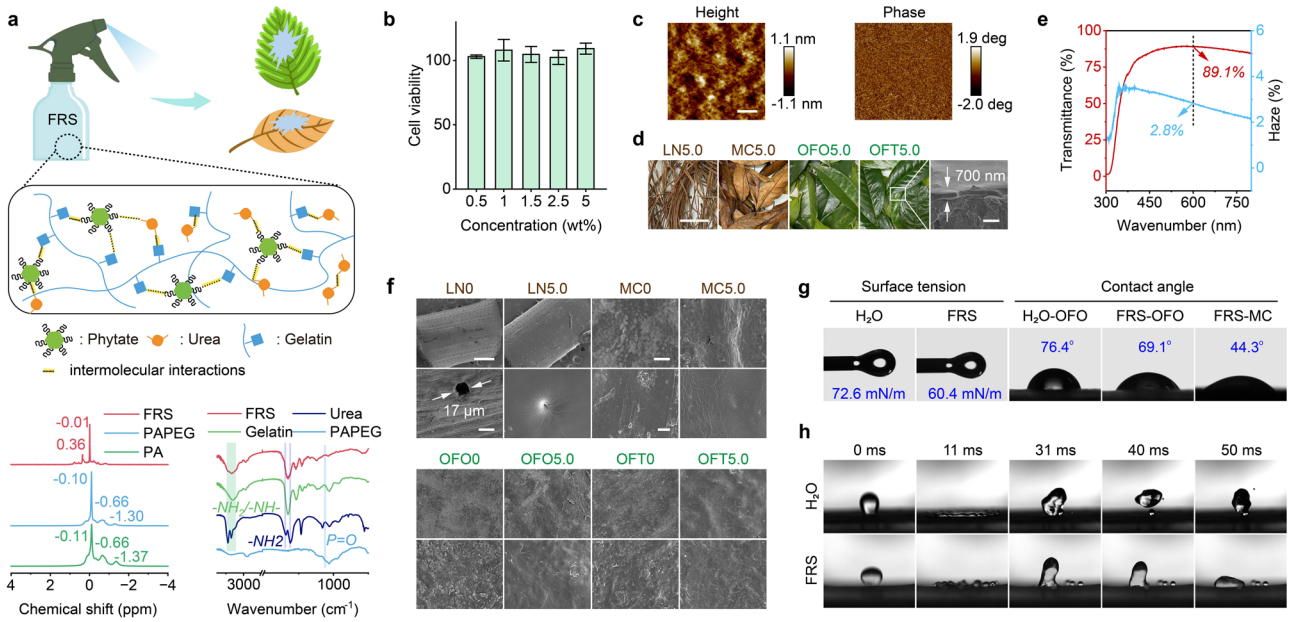

Fig. 1 | Preparation and application of FRS. a Preparation of FRS, ^{31}P NMR, and FTIR spectra. **b** The results of the cell viability test. **c** AFM images of flame-retardant coating. Scale bar, 200 nm. **d** Digital photos of leaves with 5.0 wt% FRS (scale bar, 5 cm), including larch needles (LN5.0), *Michelia chapensis* (MC5.0), *Osmanthus fragrans var. aurantiacus* (OFO5.0) and *Osmanthus fragrans var. thunbergii* (OFT5.0), and SEM image of the cross-section for OFT5.0 (scale bar, 2 μm). **e** The transparency of FRS. **f** SEM images of the surface of leaves with 0 wt% and 5.0 wt% FRS. Scale bars of LN0 and LN5.0, 500 μm and 20 μm. Scale bars of MC0, MC5.0, OFO0, OFO5.0, OFT0 and OFT5.0, 100 μm and 5 μm. **g** Results of surface tension and CA. **h** Impact behavior of H_2O and FRS on a lotus leaf.

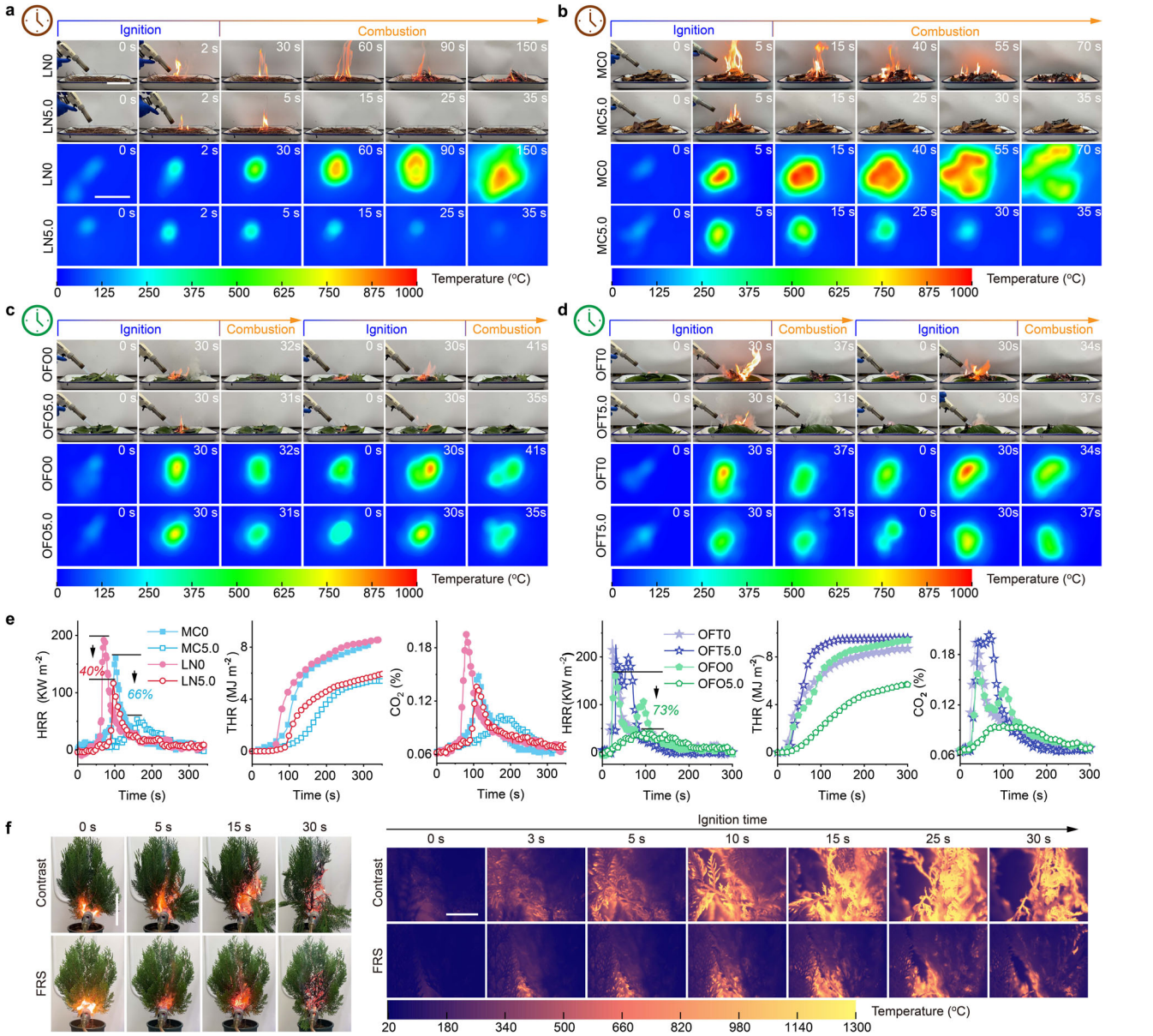

Fig. 2 | Fire resistance of leaves with FRS. a–d Digital photographs of the burning behavior at different times and along with their temperatures determined by the IR camera for LN*x* (**a**), MC*x* (**b**), OFO*x* (**c**), and OFT*x* (**d**), and where *x* represents the weight percentages of the FRS solution. Scale bar, 10 cm. **e** CCT curves of the dry leaves and fresh leaves. **f** Digital photos of the burning behavior at different times (scale bar, 15 cm) and their temperature determined by the IR camera for cypresses contrast and FRS (5 wt%) (scale bar, 3 cm).

PHRR) and fire growth index (FGI, PHRR/TTI). Correspondingly, the total heat release rate (THR) and the release of CO and CO_2 dropped significantly. There were 49% and 26% reduction in the average CO_2 yield (ACO_2P) of LN5.0 and MC5.0, respectively. In addition, lower average effective heat of combustion (AEHC) suggested incomplete combustion of volatiles due to the presence of gas-phase flame retardants[26]. Similarly, FRS retarded the ignition of fresh leaves, in addition to delaying the time to peak heat release rate (TTPHRR). For OFO5.0, the PHRR, THR, av-EHC, and release of CO and CO_2 presented dramatic decreases with respect to OFO0. However, OFT5.0 started burning at 7 s, with no reduction in THR compared with that of the uncoated gelatin-based material, eventually resulting in varying increases for the av-EHC and ACO_2P. This was probably because the leaves with lower water contents were more likely to burn completely in 40 kW m^{-2}, as evidenced by the decrease in total smoke production (TSP) and the average CO yield (ACOP). In general, the use of FRS endowed fresh and dry leaves with better anti-ignitability and flame retardancy. Spraying FRS on the cypress as a flammable tree also inhibited the burning of branches and greatly reduced the heat release from tree combustion, and the burning area was small when the contrast sample had basically burned out (Supplementary Movie 5 and Fig. 2f).

Flame-retardant mechanism

Therefore, why does FRS help self-extinguish leaves, slow the spread of fire, and reduce heat release? We conducted further research. In Fig. 3a, the spray-treated leaves presented darker residual charcoal after combustion with sufficient oxygen, especially the fallen leaves, suggesting that the coating also left char behind or promoted carbonization of the leaves. In contrast to pure gelatin, the combination of the gelatin-PAPEG-urea coating produced a denser char layer, as shown in Fig. 3b, and it displayed a coking charred layer with bubbles on the inner surface of the hybrid coating. This char layer can form on the surfaces of LN5.0 and OFO5.0, thereby preventing the release of heat or volatiles during combustion, leading to rapid temperature reduction and inhibition of further burning. Raman spectroscopy of the combustion residues revealed a clear D peak

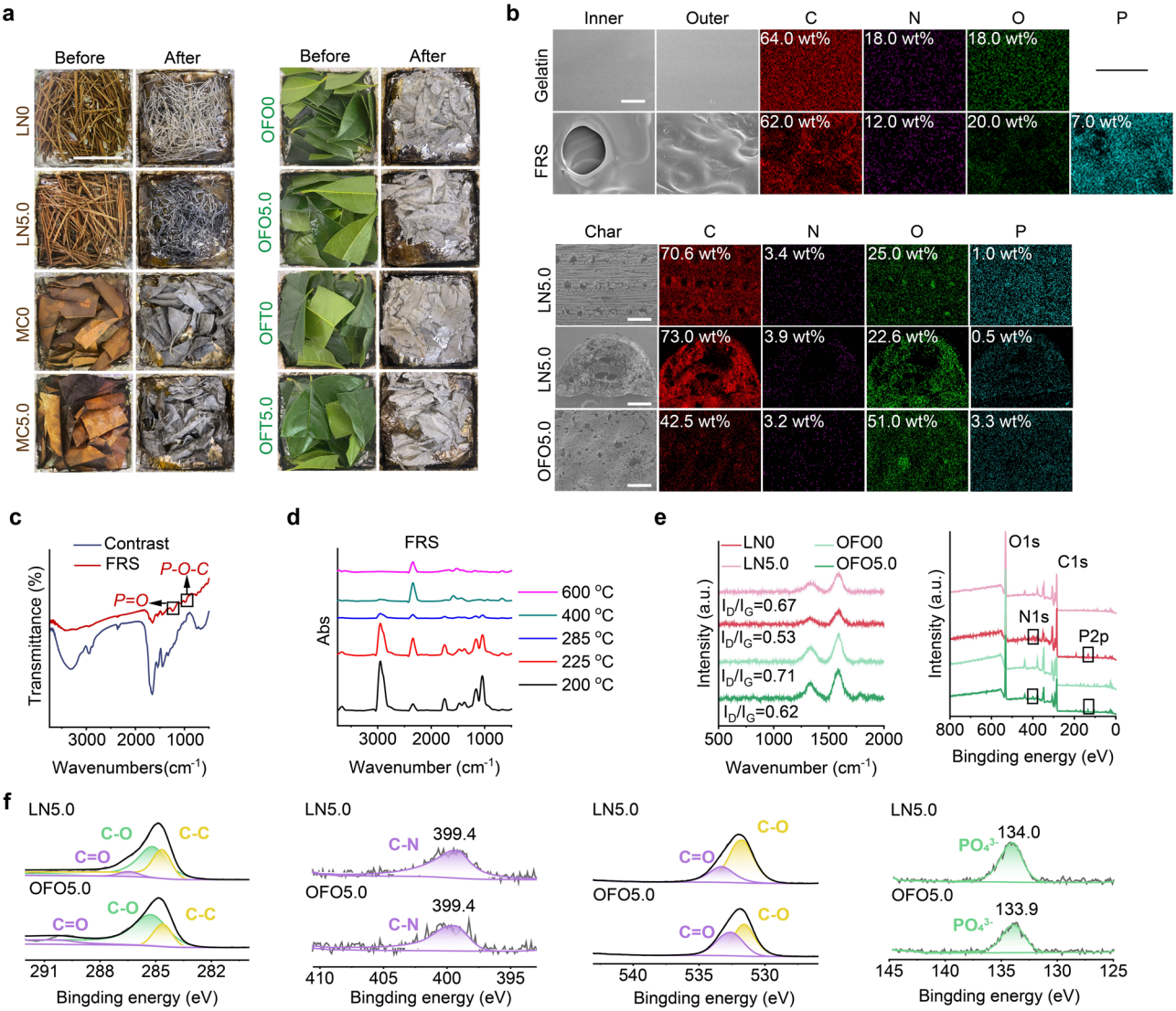

Fig. 3 | Flame-retardant mechanism of FRS. a Digital photos of the fresh and dry leaves before and after CCT. Scale bar, 5 cm. **b** Micro-morphologies of char and element distribution maps for gelatin and FRS (scale bar, 100 μm), and the leaves (scale bar, 100 μm). **c** FTIR spectra of char. **d** FTIR spectra of volatiles at different temperatures. **e** Raman curves and full survey XPS data for the char. **f** High-resolution spectra.

(1350 cm^{-1}) and G peak (1580 cm^{-1}) in the char (Fig. 3e), and the I_D/I_G ratios of LN and OFO in the FRS samples were lower than those in pure samples, indicating the greater graphitization. We subsequently conducted an in-depth analysis of its chemical structure. The EDS results indicated the existence of phosphoric acid compounds, as evidenced by the presence of 7 wt% phosphorus, which increased the amount of oxygen on the residue's outer surface, and phosphorus was also detected on the leaf surface after combustion. The signals of the P=O and P–O–C group at 1248 cm^{-1} and 996 cm^{-1} were detected in the FTIR spectra of the FRS (Fig. 3c). For the residual carbon of leaves, the peaks of PO_4^{3-} at 134.0 eV and 133.9 eV were detected in the P2p spectrum, and fresh leaves had a higher oxidized carbon content than dry leaves did in the C1s spectrum, resulting in lower graphitization (Fig. 3f). It is hypothesized that phosphoric acid and polyphosphoric acid pyrolyzed from PA were involved in the carbonization process and greatly improved the char yield and its thermal stability[20,27]. It means that promoted carbonization prevented further combustion of the material, while also inhibiting the release of smoke and heat.

In the gas phase, the composition of volatiles released by FRS from 200 °C to 600 °C was analyzed via TG-FTIR. As shown in Fig. 3e, the peak positions of the degradation products were mainly concentrated in several bands: 3300–3750 cm^{-1}, 2800–3000 cm^{-1}, 2200–2400 cm^{-1}, 1700–1800 cm^{-1}, 1300–1600 cm^{-1}, and 1000–1250 cm^{-1}. Given the chemical structure of flame retardant and gelatin, the peak at 2800–3000 cm^{-1} corresponded to the vibrational absorption peaks of small molecular aliphatic hydrogen, such as $-CH_2-$ and =CH–. The peaks at 2200–2400 cm^{-1} were the vibrational absorption peaks of CO_2 and C≡N, and those at 1700–1800 cm^{-1} were the vibrational absorption peaks of carbonyl groups. The peaks at 1300–1600 cm^{-1} belonged to the absorption peaks of C=C, C=N, and C–N, and those at 1000–1250 cm^{-1} were the absorption peaks of P=O, P–O–C, C–O, and NH_3. The P=O and P–O–C would further decompose to PO· and PO_2· to promote the termination of the combustion chain reaction and quench the burning, thus delaying leaf combustion and leading to rapid self-extinguishment and a decrease in burning temperature[14,28]. The gelatin was pyrolyzed to alkane volatiles, and like urea, it simultaneously released nitrogenous gases that can dilute the concentration of flammable gases to inhibit burning[21,29,30]. This is why the AEHC was lower and could self-extinguish during combustion.

Fertilizer application

Where will the spray go when the fire protection is lifted, such as when it rains under dry conditions? Urea, a key component of FRS, serves not only as a soil fertilizer but also as a foliar fertilizer and is directly absorbed by plant

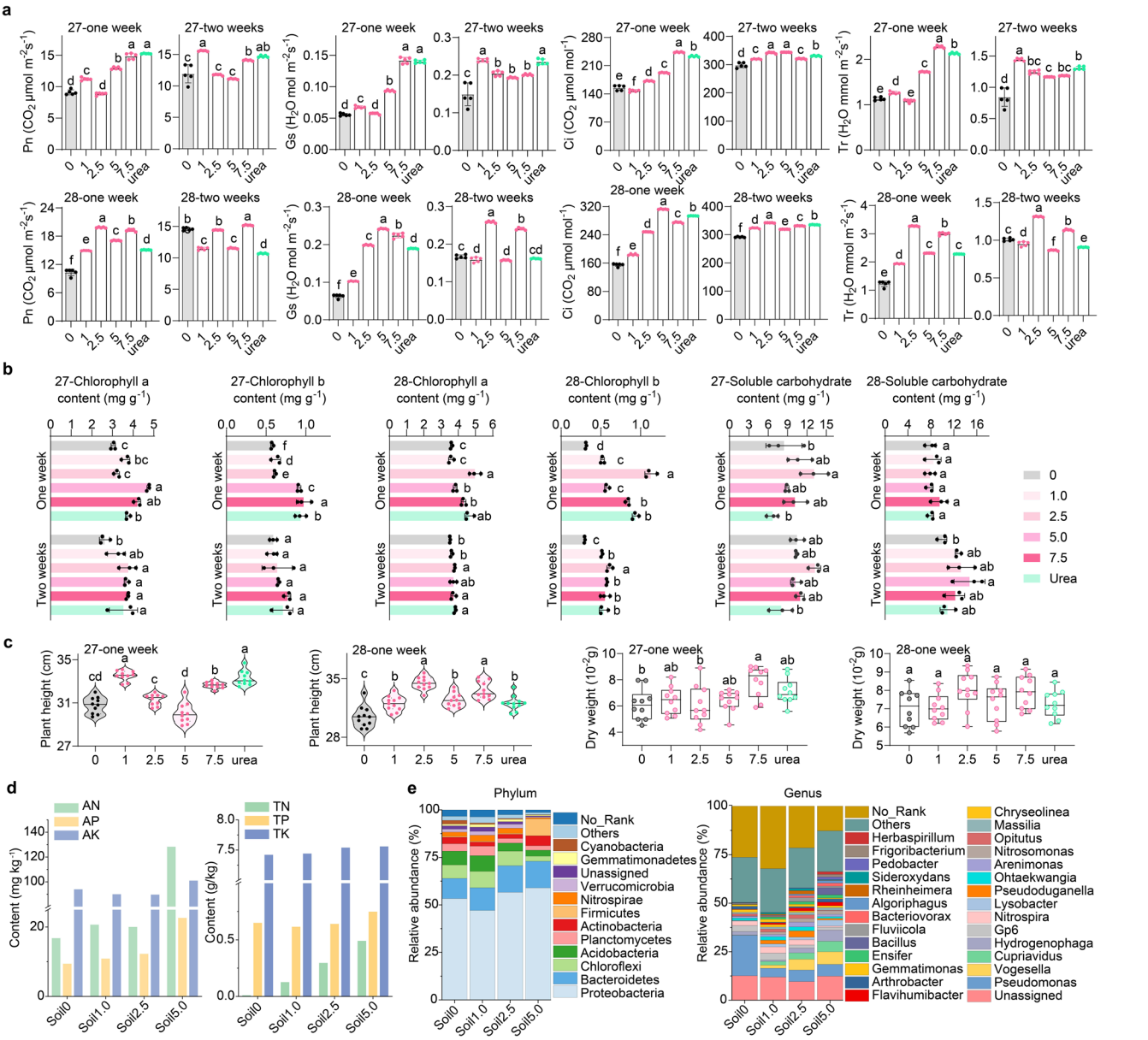

Fig. 4 | Effects of the FRS on plant growth and soil properties. a Comparison of net photosynthetic rate (Pn), leaf stomatal conductance (Gs), intracellular CO_2 concentration (Ci), and transpiration rate (Tr) in different wheat leaves ($n = 5$). **b** Comparison of chlorophyll a, chlorophyll b, and soluble sugar contents in different wheat leaves ($n = 3$). **c** Comparison of the plant height and dry weight of different wheat varieties ($n = 10$). **a**–**c** $P < 0.05$, one-way ANOVA. **d** Chemical properties of soils with different FRS concentrations. **e** Soil bacterial community composition at the phylum and genus levels.

leaves. Therefore, the harmless coating sprayed on the leaves would be absorbed by the trees as fertilizer and promote their growth in a humid environment. This was demonstrated in wheat seedlings (Yangmai-27 and Yangmai-28, *Triticum aestivum* L.). The FRS promoted the photosynthetic rate of leaves rather than inhibiting it (Fig. 4a). Especially for the first week, the Pn of wheat treated with 7.5% FRS increased by 63% and 84%, respectively. Even the effect was better than that in the samples treated with 1.25% urea alone, where Yangmai-28 showed a 28% enhancement. The FRS continued to be effective in the second week, unlike Yangmai-28, those samples were treated only with urea, indicating its slow-release properties. This may be due to the interaction of urea with phosphates and gelatin in the coating, which prevents the volatilization of urea in the air[31–33]. Similarly, as a major component of the photosystem, the contents of chlorophyll a and chlorophyll b were increased to varying degrees (Fig. 4b).

In addition, there was a slight increase in soluble sugars and protein inside the leaves after FRS treatment (Fig. 4b and Supplementary Fig. 4a). The H_2O_2 and malondialdehyde (MDA) contents were not significantly elevated, indicating that no peroxidation damage occurred (Supplementary Fig. 4a). Therefore, the FRS markedly promoted plant growth in terms of plant height and weight of materials (Fig. 4c and Supplementary Fig. 4b). After one week, the wheat in the 7.5% FRS treatment were 2.5 cm and 3.2 cm greater than that in the control group, respectively. There were 5–28% and 5–14% heavier weights of dry matter at various FRS concentrations.

If it rains, the coating will be washed off from the leaves and eventually run into the soil. The fertilizer release of FRS in the soil and its effect on soil microorganisms should also be further researched. In Fig. 4d, the available nitrogen (AN) and total nitrogen (TN) contents significantly increased with increasing the FRS concentration, where the AN content of Soil5.0 increased to 111.5 mg kg^{-1}, a 664% increase compared with that of Soil0. This is not only because of the fertility provided by urea but also because of the possible degradation of gelatin. Notably, the available phosphorus (AP) and total phosphorus (TP) stepped up as concentration increases. There were 140%

and 15% boosts in the AP and TP of Soil5.0, respectively, illustrating that phytate may be degraded by soil microorganisms to phosphate compounds that were taken up by rhizomes. Although the bacterial abundance decreased with increasing FRS, it did not disrupt the basal metabolism, environmental response, and adaptation of the soil (Supplementary Fig. 5a, b). In Fig. 4b, at the phylum level, the main dominant categories included *Proteobacteria*, *Bacteroidetes*, and *Chloroflexi*, with the relative abundances of *Proteobacteria* and *Bacteroidetes* in Soil5.0 increasing by 5.6% and 3.3%, respectively, compared with those in Soil0. Interestingly, the abundance of *Firmicutes* increased by 8.4%. Furthermore, at the genus level, there was a substantial reduction in *Pseudomonas* in Soil5.0 compared with Soil0, while *Vogesella* and *Cupriavidus* increased from 0% in Soil0 to 6.5% and 5.4% in Soil5.0, respectively. The heat map indicated the distribution of colonies (Supplementary Fig. 5c, e). The correlations between environmental factors and microbial colonies were further investigated (Supplementary Fig. 5d, f). Overall, the FRS provided the soil with nitrogen and phosphorus fertilizers and promoted the distribution of the corresponding colonies (e.g., nitrogen-fixing bacteria) without effect on the basic functions of soil.

Conclusion

We have demonstrated that simple surface modification can effectively enhance forest fire resistance. During combustion, the FRS formed a char layer on the leaf surface, acting as a barrier to oxygen and heat, and decomposed in the gas phase to produce phosphorus-containing radicals, which quenched reactions and inhibited the combustion of both fresh and dry leaves. This resulted in reduced heat release, a smaller combustion area, and rapid cooling. Additionally, the degraded coating promoted plant growth without disrupting soil microbial functions. However, practical application reveals limitations in this work, such as the susceptibility of gelatin to degradation and inadequate smoke suppression. In future work, we will address FRS's long-term storage stability and improve its smoke suppression ability.

Method

Materials

The following materials were used in the experiment: phytic acid (PA, 70% aqueous solution, Aladdin), polyethylene glycol 200 (PEG200, Macklin), gelatin (250 g Bloom, Aladdin), urea (99.5%, Aladdin), and deionized water (H_2O). All chemicals were used directly without additional purification. Larch needles (LN, 18.2% moisture content), fallen leaves with *michilia chapensis* (MC, 20.2% moisture content), *Osmanthus fragrans var. aurantiacus* leaves (OFO, 47.3% moisture content), *Osmanthus fragrans var. thunbergii* leaves (OFT, 44.6% moisture content) and soil were obtained from the campus of Zhejiang University, China. Potted cypresses (~50 cm high), which are flammable trees, were obtained from Guangdong Province, China. Plywood (100 mm × 100 mm × 5 mm), 304 steel plates (100 mm × 100 mm × 3 mm), and glass (50 mm × 50 mm × 4 mm) were wiped with ethanol before use.

Synthesis of PAPEG

PAPEG was synthesized via an esterification reaction between PA and PEG200. In brief, phytic acid (13.2 g, 14 mmol) and PEG200 (16.8 g, 84 mmol) were added to the flask under nitrogen gas. The system was stirred at 50 °C for 1 h, after which the mixture was incubated at 130 °C for 5 h to obtain the dark brown product PAPEG. Because esterification was nearly complete, PAPEG can be used directly without requiring additional purification.

Convenient preparation of a gelatin-based precursor and a flame-retardant spray (FRS) for leaves and cypresses

The gelatin-based precursor was prepared by mixing gelatin, urea, PAPEG, and H_2O in various amounts. Gelatin was dissolved in H_2O at 50 °C, subsequently urea and PAPEG were added, and the mixture was stirred well for 10 min. The solution was scraped onto the surface of plywood and steel plates and then cured at 40 °C. This process was repeated several times until the thickness of cured coatings reached 0.4 ± 0.02 mm. The system (1:0.5:0.5 of gelatin, PAPEG, and urea) was prepared with 2.5 wt% and 5.0 wt% aqueous solutions to obtain FRSs, which were sprayed on the leaves and cypresses by using an airbrush (101 W, 1.5 mm nozzle orifice) with a 2.5 bar spray pressure and distance of 12 cm. Finally, the samples were left to dry at room temperature. For 30 g of flat leaves, 30 g of FRS solution was used. Blank samples were prepared by spraying with 30 g of H_2O according to the method above. The fire-resistant leaves were named LN*x*, MC*x*, OFO*x*, and OFT*x*, and *x* represent the weight percentages of FRS solution. For each cypress, 30 g of FRS (5 wt%) solution was used.

General characterization

FTIR spectra were recorded on the Nicolet iS50 instrument (Thermo Fisher CO., USA). ^{31}P NMR spectra were obtained on DMX-500 spectrometer (BRULCER CO. Switzerland) in D_2O. X-ray photoelectron spectroscopy (XPS) was measured on Escalab 250Xi spectrometer (Thermo Fisher Scientific, UK). The contact angle (CA) of leaves and liquid surface tension of samples were obtained on an OCA 20 measuring device (Dataphysics CO., Germany) at ambient temperature, and the volumes of water were set at 3.5 μL for CA measurement. Transmittance and haze of the coatings were obtained on Cary5000 ultraviolet-visible spectrophotometer (Agilent Technologies Co. Ltd., USA), by testing the coated glass with the thickness of 0.1 ± 0.02 mm. Atomic force microscopy (AFM) images were acquired by a VeecoMultiMode AFM microscopy in tapping mode with a scanning rate of 1.0 Hz. Scanning electron microscopy (SEM) was performed on a SU-3500 instrument (Hitachi, Japan) at a voltage of 20 kV, and it coupled with X-max20 energy dispersive X-ray spectroscopy (EDS) (Oxford Instruments, UK) to analyze element compositions. The cone calorimeter test (CCT) was measured with a cone calorimeter (FTT, UK) in accordance with the ISO5660-1 standard procedures, and a heat flux used for fallen leaves (LN, MC), fresh leaves (OFO, OFT), and plywood with FRS were 20, 40 and 50 kW m^{-2}, respectively. The amount tested for dried leaves and fresh leaves were about 5 g and 10 g, which were placed uniformly in square test trays with side lengths of 100 m, not exceeding 50 mm in height. The thermogravimetric analyzer (TGA) was recorded on TA-Q500 (TA CO. USA) from 50 °C to 800 °C at the heating rate of 10 °C min^{-1} under an air atmosphere with 50 ml min^{-1} flow. TGA coupled with FTIR (TG-IR) tests were performed at a heating rate of 20 °C min^{-1} from 50 °C to 800 °C under nitrogen. FTIR sample cell was maintained at 280 °C. The Raman spectra of the residue char were recorded with a DXR532 laser Raman spectrum analyzer (Thermo Fisher, USA).

Moisture content test

The leaves (m_1) were packed in kraft paper envelopes (m_2) and placed in the oven at 105 °C for 12 h. And then the leaves and envelopes (m_3) were weighed immediately to calculate the moisture content [MC (%)] of the leaves via the following formulas.

$$\mathrm{MC}(\%) = \frac{(m_1 + m_2) - m_3}{m_1} \times 100\%$$

Drop impact on the leaf surface

H_2O and FRS droplets (27 μL) were delivered via a tiny tube on the lotus leaf surface with an impact velocity of 2.7 m s^{-1}, and on the OFO leaf surface with an impact velocity of 5.0 m s^{-1}.

Cell viability assay

A Cell Counting Kit-8 (CCK-8) assay was used to assess the viability of L929 cells cultured with different extracts. 100 μL L929 cells (5000 cells) were inoculated onto 96-well plates and cultured for 24 h until the cells were attached to the wall. A total of 100 μL of culture solution containing FRS (0.5, 1.0, 1.5, 2.5, 5.0 wt%) was added to each well, and the control group was the culture mixture without FRS and the cells were incubated for 48 h.

Subsequently, 10 μL of CCK-8 was added to each well, and the 96-well plate was removed after 3 h of incubation. The OD value of each well at 450 nm was detected with an enzyme marker.

Burning test for the leaves

The homemade combustion device was used to study the flame retardancy of leaves. The vertical infrared camera (IR camera) and horizontal camera were 75 cm and 40 cm away from the samples, respectively. For cypresses combustion, the infrared camera (IR camera) on the left and the camera in the front were 25 cm and 40 cm away from the samples, respectively.

Determination of soil environmental factors

Each portion of soil (200 g) was sprayed with 10 ml of FRS aqueous solution at different concentrations (0, 1.0, 2.5, 5.0 wt%) and collected in brown soil sampling bottles, which were named Soil0, Soil1.0, Soil2.5, and Soil5.0. Then, the soil was left in a dark place for one week at room temperature for the test.

Analysis of soil microorganisms

The test was conducted through relative quantitative sequencing of microbial 16S amplicons. DNA integrity was detected using agarose gel electrophoresis, and DNA concentration and purity were measured by a Nanodrop 2000c spectrophotometer (Thermo Fisher Scientific, USA). Then, samples were amplified for PCR amplification of the target region through V4-V5 region-specific primers (F = Illumina adapter sequence 1 + GTGCCAGCMGCCGCGG, R = Illumina adapter sequence 2 + CCGTCAATTCMTTTRAGTTT). And the introduction of specific index sequences to the library was ended by high-fidelity PCR using primers with index sequences. The library quality check was conducted after library quantification and pooling. Finally, the libraries were sequenced by the NovaSeq 6000 with the double-ended sequencing strategy of SP-Xp (PE250).

The adapter sequences and primers of raw data were removed by the cut adapt plug-in of QIIME2 software (Quantitative Insights Into Microbial Ecology pipeline V1.8.0). Data were quality filtered, noise reduced, spliced, and dechimerized via the DADA2 plug-in for QIIME2 and Usearch software, and feature tables and representative sequences were generated. The high-quality sequences were clustered by means of the Usearch software to obtain operational taxonomic units (OTUs). R package was utilized to analyze t multi-sample species composition in the community.

Plant materials and experiments

Two common wheats (Yangmai-27 and Yangmai-28, *Triticum aestivum L.*) were grown under 14 h light at 23 °C and 10 h dark at 15 °C in an automatic controlled greenhouse at Huajiachi Campus, Zhejiang University, Hangzhou, China. And the experiment was conducted in groups of four pots and designed with three replications and a random arrangement. The seedlings thinned to 7 per pot after ten days of seed germination. The treatments were conducted starting from the two-leaf stage, and seedlings were sprayed with different concentrations of FRS (0, 1.0, 2.5, 5.0, and 7.5 wt %) and 1.25% aqueous urea solution at 10 ml per pot at am 8:00, respectively. Wheat was sampled and tested one week and two weeks after treatment.

The photosynthetic parameters of net photosynthetic rate (Pn), leaf stomatal conductance (Gs), intracellular CO_2 concentration (Ci), and transpiration rate (Tr) were tested by LI-6400XT Photosynthesis meter (Licor, USA). The air temperature, relative humidity, CO_2 concentration and photosynthetic photon flux density were maintained at 20 °C, 75%, 440 μmol·mol^{-1}, and 1000 μmol·m^{-2}·s^{-1}. Chlorophyll a and b (the absorbance at 645 nm and 663 nm), soluble sugar (the absorbance at 630 nm), soluble protein (the absorbance at 595 nm), H_2O_2 (the absorbance at 390 nm), and malondialdehyde (MDA) (the absorbance at 532 nm and 600 nm) content of wheat leaves were conducted by M200 multifunctional enzyme marker (MDS ANALYTICAL, USA). The height, dry weight, and fresh weight of the wheat were measured manually.

Data availability

All data are available in the main text or the supplementary materials, and are also available from the corresponding author on reasonable request.

Received: 16 August 2024; Accepted: 30 November 2024;
Published online: 19 December 2024

References

1. Bowman, D. M. J. S. et al. Vegetation fires in the Anthropocene. *Nat. Rev. Earth Environ.* **1**, 500–515 (2020).
2. Powell, L. L. et al. The last Afromontane forests in Angola are threatened by fires. *Nat. Ecol. Evol.* **7**, 628–629 (2023).
3. Cascio, W. E. Wildland fire smoke and human health. *Sci. Total Environ.* **624**, 586–595 (2018).
4. Kelly, L. T. et al. Fire and biodiversity in the Anthropocene. *Science* **370**, eabb0355 (2020).
5. Frelich, L. E. Wildland fire: understanding and maintaining an ecological baseline. *Curr. For. Rep.* **3**, 188–201 (2017).
6. Bowman, D. M. J. S. et al. Fire in the earth system. *Science* **324**, 481–484 (2009).
7. Xu, R. et al. Global population exposure to landscape fire air pollution from 2000 to 2019. *Nature* **621**, 521–529 (2023).
8. Statistical Bulletin of the People's Republic of China on National Economic and Social Development, 2023. https://www.stats.gov.cn/sj/zxfb/202402/t20240228_1947915.html (2024).
9. Gnusov, M. A., Popikov, P. I., Malyukov, S. V., Sherstyukov, N. A. & Pozdnyakov, A. K. Improving the efficiency of forest fire prevention and suppression with of forest fire machine. *IOP Conf. Ser. Mater. Sci. Eng.* **919**, 032025 (2020).
10. Mosina, K. S. et al. Alumina nanoparticles for firefighting and fire prevention. *ACS Appl. Nano Mater.* **3**, 4386–4393 (2020).
11. Hesseln, H. Wildland fire prevention: a review. *Curr. For. Rep.* **4**, 178–190 (2018).
12. Zhao, H. et al. Trophic transfer of organophosphorus flame retardants in a lake food web. *Environ. Pollut.* **242**, 1887–1893 (2018).
13. Daniel, G., Silva, A. R. R., de Souza Abessa, D. M. & Loureiro, S. Fire suppression agents combined with gasoline in aquatic ecosystems: a mixture approach. *Environ. Toxicol. Chem.* **40**, 767–779 (2020).
14. Liu, B. W., Zhao, H. B. & Wang, Y. Z. Advanced flame-retardant methods for polymeric materials. *Adv. Mater.* **34**, 2107905 (2022).
15. Puri, R. G. & Khanna, A. S. Intumescent coatings: a review on recent progress. *J. Coat. Technol. Res.* **14**, 1–20 (2017).
16. Jiang, Y. et al. Surface flame-retardant systems of rigid polyurethane foams: an overview. *Materials* **16**, 2728 (2023).
17. Naiker, V. E., Mestry, S., Nirgude, T., Gadgeel, A. & Mhaske, S. T. Recent developments in phosphorous-containing bio-based flame-retardant (FR) materials for coatings: an attentive review. *J. Coat. Technol. Res.* **20**, 113–139 (2023).
18. Joseph, P., Bakirtzis, D., Richard, Q. & Brulfert, R. In *6th International Conference on Materials Processing and Characterization (ICMPC)* 5282-5289 (Materials Today: Proceedings, 2017).
19. Yu, A. C. et al. Wildfire prevention through prophylactic treatment of high-risk landscapes using viscoelastic retardant fluids. *PNAS* **116**, 20820–20827 (2019).
20. Zhang, J., Li, Z., Zhang, L., Yang, Y. & Wang, D. Y. Green synthesis of biomass phytic acid-functionalized Uio-66-NH_2 hierarchical hybrids toward fire safety of epoxy resin. *ACS Sustain. Chem. Eng.* **8**, 994–1003 (2020).
21. Li, Y. et al. Lignocellulose nanofibril/gelatin/MXene composite aerogel with fire-warning properties for enhanced electromagnetic interference shielding performance. *Chem. Eng. J.* **431**, 133907 (2022).
22. McDowell, R. W. & Stewart, I. Peak assignments for phosphorus-31 nuclear magnetic resonance spectroscopy in pH range 5-13 and their application in environmental samples. *Chem. Ecol.* **21**, 211–226 (2005).

23. He, L. et al. Extra strong Cu^{2+}-doped intumescent char to protect epoxy resin against fire. *Compos. Part B* **253**, 110539 (2023).
24. Liu, Y. et al. Phosphate-based covalent adaptable networks with recyclability and flame retardancy from bioresources. *Eur. Polym. J.* **144**, 110236 (2021).
25. Hou, Y. et al. Superior hard but quickly reversible si-o-si network enables scalable fabrication of transparent, self-healing, robust, and programmable multifunctional nanocomposite coatings. *J. Am. Chem.* **144**, 436–445 (2022).
26. Jian, R., Wang, P., Xia, L. & Zheng, X. Effect of a novel P/N/S-containing reactive flame retardant on curing behavior, thermal and flame-retardant properties of epoxy resin. *J. Anal. Appl. Pyrolysis* **127**, 360–368 (2017).
27. Zilke, O., Plohl, D., Opwis, K., Mayer-Gall, T. & Gutmann, J. S. A flame-retardant phytic-acid-based lbl-coating for cotton using polyvinylamine. *Polymers* **12**, 1202 (2020).
28. Sai, T., Ran, S., Guo, Z., Song, P. & Fang, Z. Recent advances in fire-retardant carbon-based polymeric nanocomposites through fighting free radicals. *SusMat* **2**, 411–434 (2022).
29. Wang, Y. T. et al. Green approach to improving the strength and flame retardancy of poly(vinyl alcohol)/clay aerogels: incorporating biobased gelatin. *ACS Appl. Mater. Interfaces* **9**, 42258–42265 (2017).
30. Zhu, F., Chen, L. & Feng, Q. Waste gelatin based layer by layer assembly for sustainable solution to cotton fabrics flame retardancy. *Prog. Org. Coat.* **163**, 106688 (2022).
31. Su, H. et al. Enhancing bioavailability of fertilizer through amyloid-like protein coating. *Adv. Mater.* **35**, 2300829 (2023).
32. Liang, D., Shi, H., Lu, Q., Quirino, R. L. & Zhang, C. Controlled-release fertilizers with an ultralow coating content. *J. Mater. Chem. A* **11**, 4527–4538 (2023).
33. Chen, X. et al. Producing more grain with lower environmental costs. *Nature* **514**, 486–489 (2014).

Acknowledgements

This work was supported by the National Natural Science Foundation of China (No. 52373108). We are grateful to Dr. Yangfan Lu (School of Materials Science and Engineering, Zhejiang University) for her help with XPS measurement and analysis.

Author contributions

Conceptualization: K.C., Y.A., and H.L. Experimental investigation: Y.A., N.Z., W.L., P.Y., X.W., Y.T., C.W., Z.L., F.Z., N.Y., and J.L. Data analysis: Y.A., N.Z., W.L., Y.T., H.L., L.T., and C.H. Manuscript writing: Y.A., H.L., and K.C. Project administration: K.C.

Competing interests

The authors declare no competing interests.

Additional information

Supplementary information The online version contains supplementary material available at https://doi.org/10.1038/s43246-024-00712-z.

Correspondence and requests for materials should be addressed to Heyang Liu or Kun Cao.

Peer review information *Communications materials* thanks Ravindra G. Puri and the other, anonymous, reviewer(s) for their contribution to the peer review of this work. Primary Handling Editors: Jet-Sing Lee. A peer review file is available.